University of Groningen

Screw vs. edge dislocation strengthening in body-centered-cubic high entropy alloys and implications for guided alloy design

Baruffi, C.; Maresca, F.; Curtin, W. A.

Published in:
MRS Communications

DOI:
10.1557/s43579-022-00278-2

IMPORTANT NOTE: You are advised to consult the publisher's version (publisher's PDF) if you wish to cite from it. Please check the document version below.

Document Version
Publisher's PDF, also known as Version of record

Publication date:
2022

Link to publication in University of Groningen/UMCG research database

Citation for published version (APA):
Baruffi, C., Maresca, F., & Curtin, W. A. (2022). Screw vs. edge dislocation strengthening in body-centered-cubic high entropy alloys and implications for guided alloy design. *MRS Communications*, *12*(6), 1111-1118. https://doi.org/10.1557/s43579-022-00278-2

Copyright
Other than for strictly personal use, it is not permitted to download or to forward/distribute the text or part of it without the consent of the author(s) and/or copyright holder(s), unless the work is under an open content license (like Creative Commons).

The publication may also be distributed here under the terms of Article 25fa of the Dutch Copyright Act, indicated by the “Taverne” license. More information can be found on the University of Groningen website: https://www.rug.nl/library/open-access/self-archiving-pure/taverne-amendment.

Take-down policy
If you believe that this document breaches copyright please contact us providing details, and we will remove access to the work immediately and investigate your claim.

Downloaded from the University of Groningen/UMCG research database (Pure): http://www.rug.nl/research/portal. For technical reasons the number of authors shown on this cover page is limited to 10 maximum.

Download date: 24-01-2026

MRS Communications (2022) 12:1111–1118
© The Author(s), under exclusive licence to The Materials Research Society, 2022
https://doi.org/10.1557/s43579-022-00278-2

MRS Communications
Computational Approaches for Materials Discovery and Development Research Letter

Check for updates

Screw vs. edge dislocation strengthening in body-centered-cubic high entropy alloys and implications for guided alloy design

C. Baruffi, LAMMM, Sciences et Techniques de l'Ingénieur, École Polytechnique Fédérale de Lausanne, Lausanne 1015, Suisse
F. Maresca, Engineering and Technology Institute, University of Groningen, 9747 Groningen, The Netherlands
W. A. Curtin, LAMMM, Sciences et Techniques de l'Ingénieur, École Polytechnique Fédérale de Lausanne, Lausanne 1015, Suisse

Address all correspondence to C. Baruffi at **carolina.baruffi@epfl.ch**

(Received 2 May 2022; accepted 12 September 2022; published online: 9 November 2022)

Abstract
Body-centered-cubic (BCC) high entropy alloys (HEAs) can show exceptionally high strength up to high temperatures. Mechanistic theories are needed to guide alloy discovery within the immense multicomponent HEA compositional space. Here, two new theories for strengthening as controlled by screw and edge dislocations, respectively, are applied to predict the yield stresses of a range of BCC alloys over a wide range of temperatures. Results show that the screw theory, with one fitting parameter, can capture experiments in many dilute and non-dilute alloys while the parameter-free edge theory agrees with experiments in non-dilute alloys having a sufficiently large misfit parameter. These results indicate a transition in single-phase alloy strengthening from traditional screw dominance to edge dominance with increasing misfit that is enabled in complex non-dilute alloys. These results point to the use of the edge theory to guide design of high-temperature alloys in the non-dilute range.

Introduction
High entropy alloys (HEAs) are a new class of many-component near-random alloys having impressive mechanical properties.[1,2] Refractory body-centered cubic (BCC) HEAs in the Cr–Mo–W–V–Nb–Ta–Ti–Zr–Hf family of elements are attracting great attention because of their high-temperature strength.[3] With millions of possible compositions, the search for high-performance alloys requires guidance from physically-based theory. The traditional understanding of strength of BCC metals and alloys is based on the motion of screw dislocations, due to their very compact core structure. Recent theory and experiments suggest,[4–7] however, that some non-dilute alloys such as the multicomponent HEAs can be significantly strengthened by edge dislocations and that the shift from screw to edge control may be the origin of high-temperature strength retention.

Here, we apply the screw and edge theories of Maresca and Curtin[4,8] to a wide range of BCC alloys and probe the screw vs. edge competition that is predicted to arise in the non-dilute limit for alloys with sufficient solute misfits. Specifically, we first examine possible screw-to-edge transition in W-Ta binary alloys, for which experimental and DFT input parameters enable parameter-free predictions for both edge and screw theories. We then apply the theories to a spectrum of BCC refractory data across a broad range of temperatures, using one fitting parameter for the screw theory and no parameters for the edge theory, and the results provides further evidence for a screw-to-edge transition in strengthening mechanism. By analyzing a set of 63 refractory BCC alloys, we show that the edge theory controls strengthening if the Hume-Rothery misfit parameter δ exceeds $\sim 3.5\%$. More generally, the edge theory provides a powerful basis for predicting the yield strength of strong alloys and enables screening across the immense BCC refractory alloys space to discover the strongest high-temperature alloys.

Methods
Experimental data on yield strength for a range of alloys shown in Table II are taken from the both old and new literature.[9–14] Melting temperatures are calculated using the software ThermoCalc[15] with the TCHEA5 database.

The edge and screw strengthening mechanisms share the same theoretical framework, namely that dislocations in a random system become spontaneously wavy in order to minimize their energy.[8,16,17] Each atom, or solute, in the alloy interacts with the dislocation with an interaction energy $U^n(x_i, y_j)$ for a solute of type n at position (x_i, y_j) relative to a dislocation along z. Local chemical fluctuations, and hence energy fluctuations, along a screw dislocation lead to the spontaneous formation of kinks on different slip planes. The intersections of these kinks form cross-kinks whose failure requires the formation of point defects, thus conferring high-temperature strengthening to the alloy.[8,18] A sudden drop in strength is then typically observed above $0.5 - 0.6\ T_m$ and is associated with the activation of diffusion-controlled mechanisms that defeat the cross-kinking.[18,19] At lower temperatures, the individual kink glide motion itself is inhibited by solutes, adding to the strength.[8,17] Local chemical fluctuations along an edge dislocation cause the edge dislocation to become wavy, as it seeks to find local environments with favorable solute/dislocation interaction energies. These interaction energies are dominated by the interaction of the edge dislocation pressure field with the misfit volumes of the solutes. The wavy dislocation is then trapped in these local low-energy environments, requiring applied stress and temperature to drive dislocation motion. The fluctuating local environments in both cases establish two characteristic length scales (the waviness amplitude w_c and the length ζ_c) and a characteristic energy barrier. Strengthening is associated with a collective solute-dislocation interaction energy parameter $\Delta\tilde{E}_p$ (per unit line length) that quantifies the fluctuations in energy due to the interaction of each atomic elemental component with the dislocation.[20] For a dislocation segment of length ζ_c aligned along z and gliding a distance w_c in the x direction, the standard deviation in energy fluctuations can be expressed as

$$\sigma_{\Delta U_{tot}} = \left(\frac{\zeta_c}{\rho b}\right)^{1/2} \Delta\tilde{E}_p(w_c) \tag{1}$$

where ρb ($\rho = 1$ for screw, $\rho = 2\sqrt{2}$ for edge) is the atomic spacing along the dislocation direction, and the key quantity $\Delta\tilde{E}_p$ is

$$\begin{aligned} \Delta\tilde{E}_p(w_c) &= \left[\sum_{i,j,n} c_n \left(\Delta U_{ij}^n\right)^2\right]^{1/2} \\ \Delta U_{ij}^n &= U^n(x_i - w_c, y_j) - U^n(x_i, y_j) \end{aligned} \tag{2}$$

where c_n, $(n = 1, \ldots, N)$ are the concentrations of the alloying N elements. Computing $\Delta\tilde{E}_p$ thus requires the interaction energies U^n of each solute at all sites (i, j) around the dislocation.

For the screw dislocation, the characteristic glide distance w_c is $w_c = a$ where a is the Peierls valley spacing, corresponding to waviness at the scale of the atomic screw kinks. $\Delta\tilde{E}_p$ is difficult to obtain for the screw. First-principles results in the literature are mainly confined to binary alloys,[21] with only a few exceptions beyond the dilute limit.[22] We will use DFT results for W and Ta to study W-Ta alloys. Interatomic potentials such as the Zhou et al. potentials[23] may or may not be reasonable.[24–26] Values across a range of non-dilute alloys in the Nb–Ta–V–Ti–Zr alloys using Zhou potentials show the correct screw dislocation core range from 40 to 120 meV. Therefore, for all alloys except W-Ta, we will use $\Delta\tilde{E}_p$ as a single fitting parameter, with other material property inputs estimated as described below, to match experimental strength vs. temperature for each alloy.

For the edge dislocation, the characteristic glide distance w_c is obtained by a minimization of the total energy of the wavy dislocation. In the elasticity limit, to be used here (see below), the interaction energy is taken as $U^n(x_i, y_j) = -p(x_i, y_j)\Delta V_n$ where $p(x_i, y_j)$ is the pressure field at position (x_i, y_j) of the edge dislocation at the origin and ΔV_n is the misfit volume of the solute type n in the alloy. $\Delta\tilde{E}_p$ can then be computed in terms of the elastic constants, the dislocation core structure and pressure field (in principle computed from a Peierls-Nabarro type model), and the solute misfit volumes. Here, we will use this elasticity approximation, leading to a parameter-free theory for edge strengthening.

We stress that no theories, those discussed below or others,[26] capture the approximate plateau in yield strength versus temperature at intermediate temperatures that is frequently observed in BCC refractory HEAs.[7,27,28] The origin of this plateau is thus not understood, and is an issue for further work. Predictions here will thus not agree fully with experiments but the theories can still be useful for insight and alloy design.

Screw-controlled strengthening

A screw dislocation in a random solute environment lowers its total energy and becomes spontaneously wavy by forming atomic-scale kinks ($w_c = a$) that are spaced by an average distance $2.5\zeta_c$ where the characteristic length ζ_c is

$$\tau_b = 1.08 E_k/(ab^2\zeta_c) \tag{3}$$

where E_k is the kink formation energy. At low temperatures, the dislocation can advance by a Peierls-like motion; this is not relevant for alloys and temperatures studied here and so is not discussed. At moderate temperatures and above, the kinks glide laterally over solute-induced energy barriers, advancing the $2.5\zeta_c$ dislocation segments forward. At a temperature- and strain-rate determined enthalpy $\Delta H = kT\ln(\dot{\epsilon}_0/\dot{\epsilon})$ with $\dot{\epsilon}_0 = 10^4\ \mathrm{s}^{-1}$ a reference strain rate, the stress τ_k required to glide the kinks across the relevant energy barriers is[8,17]

$$\begin{aligned} \tau_k(\dot{\epsilon}, T) &= \tau_b + \tau_c\left[3.26\left(\frac{\Delta H}{\Delta\tilde{E}_p} - 0.06\frac{E_k}{\Delta\tilde{E}_p} + 1.07\sqrt{w_k/b}\right)^{-1} - 1.58\frac{\Delta\tilde{E}_p}{E_k}\right], \quad \tau_k > \tau_b, \\ \tau_k(\dot{\epsilon}, T) &= \tau_b - \tau_c\left[\frac{\Delta\tilde{E}_p^2}{1.59E_k^2}\left(\frac{\Delta H}{\Delta\tilde{E}_p} - 2.12\frac{E_k}{\Delta\tilde{E}_p} + 1.07\sqrt{w_k/b}\right)\right], \quad \tau_k < \tau_b. \end{aligned} \tag{4}$$

where w_k is the kink width (typically $\sim 10b$), $\tau_c = \Delta\tilde{E}_p/(ab^2)$ is a characteristic stress, and $\tau_b = 1.08E_k/(ab^2\zeta_c)$ is a back-stress-like term.

Because kinks can nucleate on different glide {110} planes along the same dislocation line, again to obtain overall lower total energy, the kinks on different planes glide and then intersect to form cross-kinks. The cross-kink spacing is $\zeta_{xk} = 7.5\zeta_c$. Advance of the screw dislocation requires breaking of the cross-kinks, which requires the formation of vacancies or self-interstitials. There is a stress $\tau_{xk,v}$ to break the vacancy cross-kinks for pinned segment lengths of $\zeta_v = 7.5\zeta_c$ that then leaves self-interstitial cross-kinks at spacing $\zeta_i = 2\zeta_v$ and requiring a stress $\tau_{xk,i}$. The strength is then the larger of these two, which are computed as[8]

$$\tau_{xk}(\dot{\epsilon}, T) = \frac{\pi E_{v/i}}{ab\zeta_{v/i}}\left[1 - \left(\frac{\Delta H}{E_{v/i}}\right)^{2/3}\right] \quad (5)$$

where $E_{v/i}$ are the vacancy and self-interstitial formation energies, respectively.

The strain-rate and temperature-dependent screw-controlled yield strength is then the sum of the above two mechanisms. The tensile yield strength is the shear strength multiplied by the Taylor factor of 2.74 for BCC screw dislocation slip in a random polycrystal, leading to

$$\sigma_y(\dot{\epsilon}, T) = 2.74(\tau_{xk}(\dot{\epsilon}, T) + \tau_k(\dot{\epsilon}, T)) \quad (6)$$

Predictions of σ_y thus require (i) the alloy Burgers vector b, (ii) the kink formation energy E_k, (iii) the vacancy and the self-interstitial formation energies $E_{v/i}$, and (iv) the solute/dislocation interaction energy parameter $\Delta\tilde{E}_p$. Here, we use $\Delta\tilde{E}_p$ as a fitting parameter, except for the W-Ta alloys. We then also use the concentrated-weighted average of the elemental properties, e.g. $\sum_1^N c_n X_n$ for properties $X = a_0, E_k, E_{v/i}$ with the elemental values estimated from experiments or first-principles.[8,29–31] All single element properties used here can be found in Table I. For Hf, Ti, and Zr, the BCC phase is unstable at low temperatures and so we use the vacancy and self-interstitial formation energies of the HCP phase and $2E_k = 1$ eV. Variations of $\pm 25\%$ in E_k and $E_{v/i}$ for these elements leads to variations of less than 5% (5 meV in the worst case) in the corresponding fitted values of $\Delta\tilde{E}_p$ and thus have no significant effect on the strength predictions.

Edge strengthening theory

The yield strength vs. temperature for the edge dislocation is computed using the analytic elasticity-based parameter-free model of Maresca and Curtin.[4] That model yields equations for the zero temperature strength and the zero temperature energy barrier as

$$\tau_{y0} = 0.040\alpha^{-1/3}\bar{\mu}\left(\frac{1+\bar{\nu}}{1-\bar{\nu}}\right)^{4/3}\left[\frac{\sum_n c_n \Delta V_n^2}{\bar{b}^6}\right]^{2/3} \quad (7)$$

$$\Delta E_b = 2.00\alpha^{1/3}\bar{\mu}\bar{b}^3\left(\frac{1+\bar{\nu}}{1-\bar{\nu}}\right)^{2/3}\left[\frac{\sum_n c_n \Delta V_n^2}{\bar{b}^6}\right]^{1/3} \quad (8)$$

where $\overline{\mu}$ and $\overline{\nu}$ are the isotropic alloy elastic constants. For later use, we highlight that the edge strengthening is driven by a collective solute misfit volume parameter that is related to the widely-used normalized misfit parameter $\delta = \sqrt{\sum_n c_n \Delta V_n^2 / 9\bar{V}^2}$ where $\bar{V}$ is the average atomic volume. Thermal activation theory then leads to the finite-temperature, finite strain rate tensile yield strength that can be well-described over a wide temperature range by the ad-hoc form

$$\sigma_y(T, \dot{\epsilon}) = 3.06\tau_{y0}\exp\left[-\frac{1}{0.55}\left(\frac{k_B T}{\Delta E_b \ln\left(\frac{\dot{\epsilon}_0}{\dot{\epsilon}}\right)}\right)^{0.91}\right] \quad (9)$$

for a random-textured polycrystalline sample where 3.06 is the Taylor factor for edge dislocation slip in BCC and α is a line-tension coefficient.

To create a computationally-efficient model, the elemental misfit volumes ΔV_n and alloy elastic constants $\bar{C}_{ij}$ are estimated using a concentration-weighted sum of the elemental values as[32]

$$\overline{C}_{ij} = \sum_{n=1}^{N} c_n C_{ij}^n; \quad \overline{V} = \sum_{n=1}^{N} c_n V_n; \quad \Delta V_n = V_n - \overline{V} \quad (10)$$

$$\overline{\mu} = \sqrt{\frac{1}{2}\overline{C}_{44}(\overline{C}_{11} - \overline{C}_{12})}; \quad \overline{B} = (\overline{C}_{11} + 2\overline{C}_{12}); \quad \overline{\nu} = \frac{3\overline{B} - 2\overline{\mu}}{2(3\overline{B} + \overline{\mu})} \quad (11)$$

with the $\bar{\mu}$ and $\bar{\nu}$ calculated using the Bacon-Scattergood relationships.[33,34] The single element properties are those given in Lee et al.[32,35] and are listed in Table I. The line tension for the BCC edge dislocation is $\Gamma = \alpha\bar{\mu}b^2$, and here we use

Table I. Single elements properties used as input to estimate the alloy properties used in the screw/edge strengthening theories (a lattice parameter; C_{ij} elastic constants; E_v vacancy formation energy; E_i self-interstitial formation energy; E_k kink formation. The latter three are estimated following Refs. 8, 29–31.

Element	Hf	Ti	Zr	Ta	W	Nb	Mo	V
a [Å]	3.55837	3.264	3.584	3.301	3.162	3.299	3.1437	3.038
C_{11} [GPa]	131	134	104	266	533	253	450	232
C_{12} [GPa]	103	110	93	158	205	133	173	119
C_{44} [GPa]	45	36	38	87	163	31	125	46
E_v [meV]	1500	1162	1275	2950	3800	2850	2900	2150
E_i [meV]	3917	2317	2845	5832	9548	5253	7417	3367
E_k [meV]	500	500	500	585	901	640	500	445

Table II. Estimated elastic constants, misfit parameter, (fitted, except for W-Ta) solute/dislocation interaction energy parameter $\Delta\tilde{E}_p$, and melting temperature for the alloys studied here.[9–12,14] Also shown is the predicted controlling strengthening mechanism (screw, edge, or mixed (edge, screw comparable).

Alloy	$\bar{\mu}$ [GPa]	$\bar{\nu}$	δ	$\Delta\tilde{E}_p$ [meV]	T_m [K]	Strengthening mech.
$W_{50}Ta_{50}$[14]	116	0.3	0.022	84	3489	Mixed
$W_{60}Ta_{40}$[14]	126	0.3	0.022	79	3529	Mixed
$W_{80}Ta_{20}$[14]	144	0.3	0.017	60	3613	Edge
$Ta_{42}Nb_{40}V_{18}$[9]	57	0.35	0.031	84	2666	Edge
$Ta_{90}Hf_1W_9$[9]	77	0.33	0.015	67	3305	Screw
$Nb_{71.7}Hf_{22.4}W_{5.9}$[9]	48	0.37	0.035	87	2471	Edge
$Nb_{68.4}Hf_{20}W_{6.4}Ta_{2.6}Zr_{2.6}$[9]	49	0.36	0.036	95	2452	Edge
$Nb_{65.6}Hf_{20}W_{9.2}Ta_{2.6}Zr_{2.6}$[9]	53	0.36	0.037	96	2456	Edge
$Nb_{90.7}Hf_{5.4}Ti_{2.6}Zr_{0.74}Ta_{0.26}W_{0.26}$[9]	43	0.38	0.028	56	2615	Screw
$Nb_{50}Ti_{50}$[10]	35	0.38	0.005	55	2206	Screw
$Nb_{39}Ti_{61}$[10]	32	0.4	0.005	65	2135	Screw
$Nb_{70}Ti_{18.1}Mo_{11.9}$[11]	51	0.37	0.015	83	2948	Screw
$Nb_{67.8}Ti_{18.1}Mo_{14.1}$[11]	53	0.36	0.016	87	2971	Screw
$Nb_{34.7}Ti_{32.5}Mo_{32.8}$[12]	67	0.34	0.021	108	2832	Screw

$\alpha = 1/6$ that is slightly larger than that used by Maresca et al.[4] but gives better overall predictions of strength vs. temperature.

Results

Material input parameters, various computed input quantities including the misfit δ parameter and the fitted $\Delta\tilde{E}_p$, for all alloys studied here are shown in Tables I and II. Table II also indicates whether our analysis below concludes that strength is controlled by screw or edge dislocations, or that both screw and edge strengths are comparable.

W-Ta alloys

To calculate $\Delta\tilde{E}_p$ for the screw dislocation, we first use DFT calculations of one single Ta at atomic positions out to 5th neighbors around a W screw core as reported by Hu et al.[8,21,36] This provides a value for the collective quantity $\Delta U^{\mathrm{Ta}} = \left[\sum_{i,j}\left(\Delta U_{ij}^{Ta}\right)^2\right]^{1/2}$ of $\Delta U^{\mathrm{Ta,dil}} = 136.9$ meV in the dilute limit. To consider the non-dilute limit, we then assume that the interaction energy changes ΔU^{Ta} and the similar quantity ΔU^{W} are

$$\begin{aligned} \Delta U^{\mathrm{Ta}} &= (1 - c_{\mathrm{Ta}})\Delta U^{\mathrm{Ta,dil}} \\ \Delta U^{\mathrm{W}} &= c_{\mathrm{Ta}}\Delta U^{\mathrm{W,dil}} \end{aligned} \tag{12}$$

where $\Delta U^{\mathrm{W,dil}}$ is the unknown interaction energy parameter for dilute W in Ta screw core. The interaction energy parameter in the non-dilute alloy is then

$$\Delta\tilde{E}_p = \sqrt{c_{\mathrm{Ta}}(1 - c_{\mathrm{Ta}})[(1 - c_{\mathrm{Ta}})(\Delta U^{\mathrm{Ta}})^2 + c_{\mathrm{Ta}}(\Delta U^{\mathrm{W}})^2]} \tag{13}$$

In the limit $c_{Ta} \to 0$, Eq. (13) equals

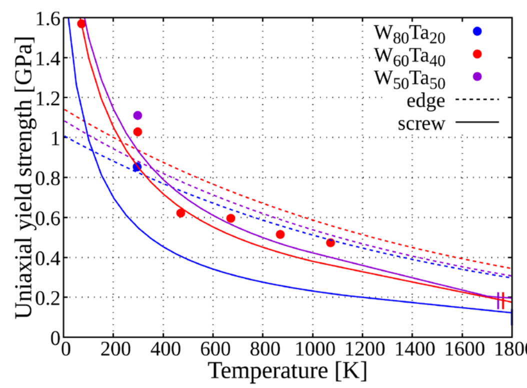

Figure 1. Uniaxial yield strength versus temperature for W-Ta alloys, as measured experimentally[14] (symbols) and as predicted using screw (solid lines) and edge (dashed line) theories.

$$\Delta\tilde{E}_p = \sqrt{c_{\mathrm{Ta}}(\Delta U^{\mathrm{Ta}})^2} \tag{14}$$

We impose Eq. (14) and (13) to be equal at $c_{\mathrm{Ta}} = 0.01$ and can then estimate $\Delta U^W = 194\ meV$. Using a smaller c_{Ta} does not change $\Delta U^W = 194\ meV$ significantly. Thus, with the assumption in Eq. (12), predictions for W-Ta alloys have no fitting parameters. Figure 1 shows the experimental yield strength for three different $W_{1-x}Ta_x$ alloys ($x = 0.2, 0.4, 0.5$)[14] along with our predicted values from the screw and edge theories at different temperatures. Reported uncertainty on specific data points is ± 70 MPa maximum.

For $W_{80}Ta_{20}$, where we can expect the $\Delta\tilde{E}_p$ to be most accurate given the available dilute-Ta DFT, the results show that the screw theory greatly underestimates the strength at room temperature. In contrast, the edge theory agrees extremely well with the measured value. Thus, this alloy appears to be edge-controlled, although more data would be necessary to draw a definitive conclusion. Increasing the Ta content to $W_{60}Ta_{40}$, we find that the low-temperature ($T = 77$K) strength is now well-predicted by the screw theory while the edge strength is increased only marginally, indicating an edge-to-screw transition at low T with increasing Ta content. With increasing temperature, however, the screw strength decreases rapidly and falls somewhat below the experiments except at 473K. The edge theory is in much better agreement with experiments at room temperature (RT), and then is somewhat larger than experiments at higher temperatures. Thus, at RT and above, screw vs. edge dominance is not clearly resolved. Neither theory matches all the experiments well, although the edge theory is more consistent overall. For comparison, fitting $\Delta\tilde{E}_p$ naturally leads to better results for the screw prediction, with $\Delta\tilde{E}_p = 85$ meV approximately 8% higher than the DFT-based estimate. Similar, modest reductions in the elastic moduli would reduce the edge prediction leading to better agreement at higher temperatures. Thus, whether the screw strength is estimated from DFT or fitted, the results highlight that screw dominance disappears and that screw and edge mechanisms become competitive. Finally, for $W_{50}Ta_{50}$ alloy, the RT strength is only slightly higher than that for the $W_{60}Ta_{40}$ alloy. The screw theory predicts such a slight increase but remains quantitatively lower while the edge theory predicts a slight decrease in strength. The predicted screw and edge strengths are then nearly identical, although both underpredict the strength. Overall, the edge theory is comparable to the data at all compositions for temperatures at or above RT, defying the common assumption that BCC alloy strengthening is always controlled by screw dislocations.

Ta and Nb-based alloys

Figure 2 shows the experimentally-measured yield strengths for (a) tantalum-based,[9] (b) niobium-based,[9] and (c) niobium-titanium alloys[10–13] (c), along with the edge predictions and screw fits; vertical lines indicate the calculated value of $0.5T_m$ for each alloy. There is limited data to indicate uncertainties in the reported measurements. These uncertainties are of the order of ±10-50 MPa for a few specific case. So, we also show experimental data on other alloys that are close in composition to indicate the expected range of experimental variations in the strength. Fitting of the screw theory is performed using only experimental data below $0.5T_m$, i.e. below temperatures where cross-kink failure may be defeated by

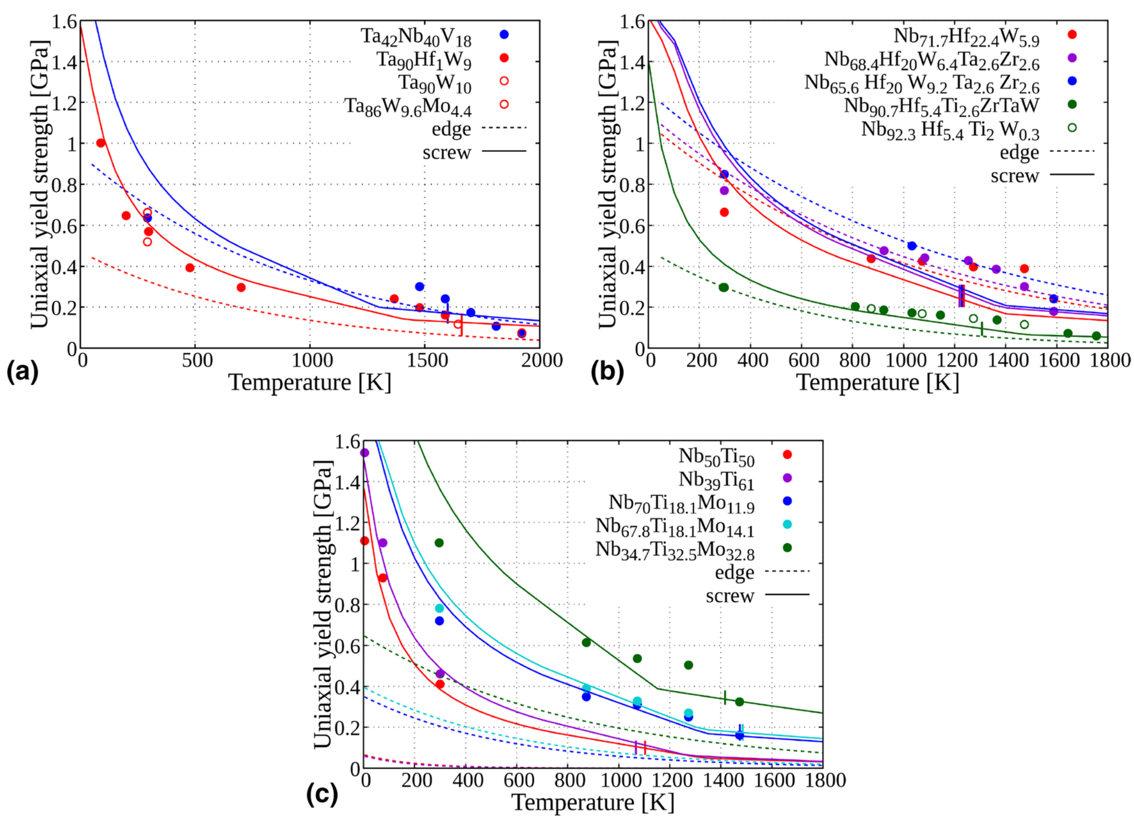

Figure 2. Experimental measurements and predictions of the uniaxial yield strength vs. temperature for (a) tantalum-based alloys,[9] (b) niobium-based alloys[9] and (c) niobium-titanium alloys.[10–13] Filled symbols indicate experiments, solid lines screw theory fitting, dashed lines edge theory predictions, open symbols data for alloys close in composition and vertical lines indicate the temperature $0.5T_m$ for each alloy, with screw fitting performed using only data below this temperature, with the exception of $Ta_{42}Nb_{40}V_{18}$ alloy where the fit is performed for data up to $T/T_m = 0.6$ due to a lack of data below $T/T_m = 0.5$.

diffusive mechanisms[19] that are not accounted for in the screw theory. The values of $\Delta\tilde{E}_p$ obtained from the fitting are shown, and also listed in Table II; experimental strength variations of 50 MPa would lead to variations of $\sim 10\%$ in the fitted $\Delta\tilde{E}_p$. The fitted $\Delta\tilde{E}_p$ values are comparable to the values estimated using Zhou potentials by Ghafarollahi et al.[17] Below, we discuss the quality of the screw-fit and edge prediction for the different alloy families.

In the Ta-based alloys[9] [Fig. 2(a)], increasing the solute concentrations yields a transition from screw-dominated to rough edge-screw equality. Specifically, for the relatively dilute $Ta_{90}Hf_1W_9$ alloy, the screw-fit captures the experiments well, especially at lower temperatures, while the edge theory is far lower than experiments. For the non-dilute, more-complex $Ta_{42}Nb_{40}V_{18}$ alloy that contains V with a large misfit vs. Ta and Nb, the edge theory is in good agreement with experiments, although slightly low at high temperature. This alloy also retains strength up to $T/T_m = 0.6$ (shown). These results again show that edge strengthening competes with screw strengthening in more complex alloys (and recalling that the screw prediction are fit to the data and so will often match the data reasonably).

Turning to the family of Nb-based alloys, Fig. 2(b) shows the experimental strengths[9] vs. temperature and the screw-fit and edge predictions for four alloys. The screw theory fit is fairly good for the dilute $Nb_{90.7}Hf_{5.4}Ti_{2.6}Zr_{0.74}Ta_{0.26}W_{0.26}$ alloy, although underestimating the yield strength around $T = 0.5T_m$, while the edge theory is much lower except at RT. For the more-concentrated alloys, however, the edge strengthening becomes competitive with the screw fit and the overall trend is better-captured by the edge theory. The edge is clearly better especially at high temperatures $T/T_m \geq 0.4$ where the screw fit is well below experimental data. The parameter-free edge theory also captures the relative strengthening of these three alloys, where the small Zr additions compensate for the slight reduction in Hf, the small Ta additions compensate for the Nb depletion, and the strengthening then comes mainly from the increasing W content. In these alloys, the strengthening also persists to somewhat above $T/T_m = 0.5$ before decreasing sharply. These overall results show that the edge dislocation can control the strength in more-complex alloys containing atoms with larger size difference (Hf, Zr, W) incorporated into a dominant medium-size-atom (Nb) matrix.

Results for Nb–Ti alloys[10–13] are shown in Fig. 2(c). For binary Nb–Ti, with data only up to RT, the edge strengthening is negligible because Nb and Ti have nearly identical sizes, and hence very small misfit volumes. The screw fit shows generally good agreement with experiments. For the more complex Mo-Nb-Ti alloys, the screw theory is again broadly good, although with larger deviations for the $Nb_{34.7}Ti_{32.5}Mo_{32.8}$. The strength also shows a decrease around $T/T_m = 0.5$, more indicative of screw control. The addition of the smaller Mo atoms to create Nb–Ti–Mo alloys[19] leads to an increasing edge strength but the predicted strength is well below experiments. These alloys are thus all expected to be screw-controlled.

Discussion

The results reported in the previous section show that the edge theory can predict the alloy strength in good agreement with experiments mainly in the higher-concentration alloys with large misfit volumes. The (fitted) screw theory can generally match experiments well, especially in the more-dilute alloys. Alloys where the edge theory agrees well may have some tendency for strength retention at higher T/T_m but not conclusively. However, these alloys can tend to have higher T_m, leading to higher-temperature capability. We thus conclude that the edge theory provides a firm physical basis for identifying high-strength/high-retained-strength BCC HEA compositions, as proposed in recent works.[32, 37] Applying the edge theory to all alloys will lead to some predictions that are very low (compared to experiments) in those alloys that are screw controlled. So, it is valuable to use our analysis and existing experimental data to identify any signatures indicating when edge strengthening is expected to dominate.

To identify a signature of edge dominance, we turn to an examination of the BCC hardness data on 63 refractory alloys aggregated by Kim et al.[14] Although hardness typically reflects the alloy strength at $\sim 10\%$ plastic strain, and hence depends not only on the yield strength but also the work hardening behavior, measuring hardness is comparatively easy. Correlating hardness with yield strength thus remains qualitatively useful. For the 63 compositions, we apply the edge theory to predict the alloy yield strength $\sigma_{y,th}$ at room temperature and nominal strain rate of $10^{-3}\,s^{-1}$, and compare to the experimental Vickers hardness H at RT. A direct comparison of H vs. $\sigma_{y,th}$ (not shown) across all 63 alloys reveals a best-fit linear correlation $H = 1.6\sigma_{y,th} + 2.86$ GPa but with a low accuracy ($R^2 = 0.47$). The slope of 1.6 is also much lower than the common value of 3 for elastic/perfectly plastic materials.[38–41] The poor correlation is due precisely to the fact that the edge theory is not applicable to all 63 alloys, i.e. some of these alloys are screw-dominated as, for instance, demonstrated in TEM on the HfNbTaTiZr alloy.[42] If the alloy is screw controlled, the edge theory underestimates the strength and fits using only the edge theory lead to small slope and high intercept.

Since the edge theory shows that edge strengthening depends mainly on the misfit parameter $\delta = \sqrt{\sum_n c_n \Delta\bar{V}_n^2/9\bar{V}^2}$, we can perform an initial screening of alloys using the criterion $\delta \geq \delta_{min}$, where δ_{min} is a threshold value. With increasing δ_{min}, fitting of the data with $\delta \geq \delta_{min}$ shows a rapid increase in the best linear fit (from $R^2 = 0.47$ to $R^2 = 0.71$) just below $\delta_{min} = 0.035$ along with an increase of the slope to 2.37. Figure 3 shows the hardness vs. predicted yield stress for all 63 alloys, but divided into those alloys with $\delta < 0.035$ (purple) and $\delta_{min} \geq 0.035$ (red). A best-fit linear line to the $\delta_{min} \geq 0.035$ data is also shown, exhibiting the higher slope and lower intercept relative to the fit (not shown) to the entire dataset. The alloys with $\delta \geq 0.035$, postulated to be edge-controlled, include all of the highest-hardness and highest-strength alloys. The alloys with $\delta < 0.035$, postulated to be screw-controlled, all have

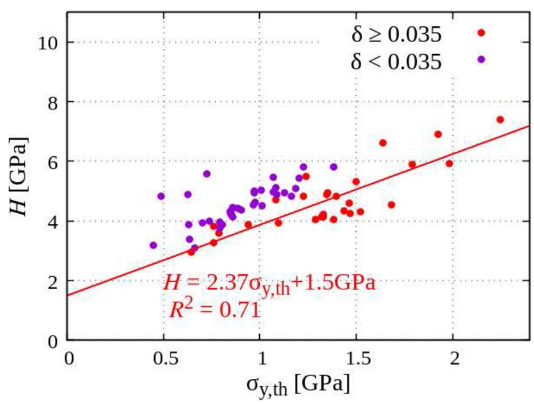

Figure 3. Experimental hardness H vs. predicted yield strength $\sigma_{y,th}$ using the edge theory, for the 63 alloys collected by Kim et al.[14] The solid red line shows a linear fit to those alloys having a misfit parameter $\delta \geq 0.035$ (red points) that are expected to be edge-controlled while the remaining alloys with $\delta < 0.035$ (purple points) are expected to be screw controlled.

hardness values above the correlation line of the edge-controlled data. This is consistent with the notion that the edge theory is a lower-bound for strength predictions.

We can further examine the viability of the criterion $\delta_{min} \geq 0.035$ by returning to the data studied earlier in this paper. Table II shows the values of δ computed for all alloys studied here. Aside from W-Ta, $\delta \geq 0.035$ is found for three of the four alloys that we independently identified as edge-controlled and the fourth alloy has $\delta = 0.031$. This supports the idea of using $\delta_{min} = 0.035$ as a criterion for discriminating between likely-edge and likely-screw controlled. Since edge strengthening also involves the elastic moduli, alloys containing high-modulus W may be edge-controlled in spite of lower δ, as seen in Table II for $W_{1-x}Ta_x$ where $\bar{\mu}$ is very high in general. The screw-edge competition in $W_{1-x}Ta_x$ is thus controlled by a combination of increasing δ and decreasing elastic coefficient with increasing Ta content.

The above results can be used for fast alloy design based on strength criteria and give theoretically-based guidelines for the selection of alloy components. Other insights emerge. For example, Nb, Ta and Ti have very similar sizes and so alloys such as $Ta_{42}Nb_{40}V_{18}$ and MoNbTi can be treated as a pseudo-binary alloys ($Nb_{82}V_{18}$, $MoNb_{67}$) with predicted strengths very close to those of the real ternary alloys. Previous screw studies found that Nb-Mo and Nb-W are also quite similar. Thus, alloy design based on the edge theory may benefit from probing a reduced compositional space by assuming Nb=Ta=Ti and/or Mo=W.

In general, the edge theory can be used fully, and should be a lower bound to the strength. Without a full calculation, however, a proposed alloy with $\delta \geq 0.035$ is likely edge-controlled and the edge theory is appropriate. If a proposed alloy has $\delta < 0.035$, then the screw theory is may be more appropriate and the hardness (and strength) can be expected to exceed the edge prediction. Edge-controlled alloys are more likely to retain strength at higher homologous temperatures. Edge-based alloy design is thus an attractive path, and has recently been pursued in work by Rao et al.[37]

Conclusions

We have made extensive comparisons of experimental alloy yield strengths vs. predictions of two recent theories for edge dislocation strengthening and screw dislocation strengthening. Although different, both theories rely on the same basic idea that dislocations in a random medium become spontaneously wavy thus inducing a strengthening effect. Results show that the alloy strength can be screw or edge dominated, depending on temperature and alloying. Typically, dilute alloys are screw dominated and edge strengthening becomes comparable to or exceeds screw strengthening in higher-concentration alloys when the misfit parameter $\delta \geq 0.035$ or when the elastic moduli are very high as in the $W_{80}Ta_{20}$ alloy. In general, the parameters entering the screw theory are challenging to compute accurately whereas the edge theory is fully predictive and relies on a few material parameters that can be easily estimated. Thus, the edge theory can always be applied and considered as a lower bound. A lower bound may miss attractive high-strength alloys, but there is no accurate approach to identifying such alloys. Attractive alloys identified using the edge analyses here can subsequently be investigated in more detail, involving more computational effort to compute the misfit volumes, elastic constants, estimates of solute/screw interaction energies, thermodynamic stability, and melting temperature. In addition, even as a lower bound, the edge theory provides a conservative strength estimate that can be useful when alloy design involves many other application constraints such as density, ductility, and oxidation resistance. The design of new alloys possessing such multi-dimensional performance needed for realistic applications is being pursued now with some success.[37]

Acknowledgments

This research was supported by the Swiss National Science Foundation through the project “Harnessing atomic-scale randomness: design and optimization of mechanical performance in High Entropy Alloys”, project “200021_18198/1” and through the NCCR MARVEL, a National Centre of Competence in Research, funded by the Swiss National Science Foundation (grant number 182892).

Declarations

Conflict of interest

The authors declare they have no conflict of interest.

References

1. D.B. Miracle, O.N. Senkov, A critical review of high entropy alloys and related concepts. Acta Mater. **122**, 448–511 (2017)
2. E.P. George, D. Raabe, R.O. Ritchie, High-entropy alloys. Nat. Rev. Mater. **4**(8), 515–534 (2019)
3. J.-P. Couzinié, O. Senkov, D. Miracle, G. Dirras, Comprehensive data compilation on the mechanical properties of refractory high-entropy alloys. Data Brief **21**, 1622–1641 (2018)
4. F. Maresca, W.A. Curtin, Mechanistic origin of high strength in refractory BCC high entropy alloys up to 1900K. Acta Mater. **182**, 235–249 (2020)
5. D. Caillard, A TEM in situ study of alloying effects in iron. II-Solid solution hardening caused by high concentrations of Si and Cr. Acta Mater. **61**(8), 2808–2827 (2013)
6. H. Yao, J. Qiao, J. Hawk, H. Zhou, M. Chen, M. Gao, Mechanical properties of refractory high-entropy alloys: Experiments and modeling. J. Alloys Compd. **696**, 1139–1150 (2017)
7. H. Chen, A. Kauffmann, S. Laube, I.-C. Choi, R. Schwaiger, Y. Huang, K. Lichtenberg, F. Müller, B. Gorr, H.-J. Christ, Contribution of lattice distortion to solid solution strengthening in a series of refractory high entropy alloys. Metall. Mater. Trans. A **49**(3), 772–781 (2018)
8. F. Maresca, W.A. Curtin, Theory of screw dislocation strengthening in random BCC alloys from dilute to "High-Entropy" alloys. Acta Mater. **182**, 144–162 (2020)
9. W.C.A. Corporation, Columbium, Tantalum and Tungsten Alloys—Technical Informations
10. D. Read, Metallurgical effects in niobium-titanium alloys. Cryogenics **18**(10), 579–584 (1978)
11. O. Senkov, S. Rao, T. Butler, T. Daboiku, K. Chaput, Effect of Fe additions on the microstructure and properties of Nb-Mo-Ti alloys. Int. J. Refract. Met. Hard Mater. **89**, 105221 (2020)
12. O. Senkov, S. Rao, T. Butler, K. Chaput, Ductile Nb alloys with reduced density and cost. J. Alloys Compd. **808**, 151685 (2019)
13. F. Wang, G.H. Balbus, S. Xu, Y. Su, J. Shin, P.F. Rottmann, K.E. Knipling, J.-C. Stinville, L.H. Mills, O.N. Senkov, Multiplicity of dislocation pathways in a refractory multiprincipal element alloy. Science **370**(6512), 95–101 (2020)
14. I.H. Kim, H.S. Oh, K.S. Lee, E.S. Park, Optimization of conflicting properties via engineering compositional complexity in refractory high entropy alloys. Scr. Mater. **199**, 113839 (2021)
15. J.-O. Andersson, T. Helander, L. Höglund, P. Shi, B. Sundman, Thermo-Calc & DICTRA, computational tools for materials science. Calphad **26**(2), 273–312 (2002)
16. C. Varvenne, A. Luque, W.A. Curtin, Theory of strengthening in FCC high entropy alloys. Acta Mater. **118**, 164–176 (2016)
17. A. Ghafarollahi, W.A. Curtin, Screw-controlled strength of BCC non-dilute and High-Entropy alloys. Acta Materialia, 117617 (2022)
18. R.R. Eleti, N. Stepanov, N. Yurchenko, S. Zherebtsov, F. Maresca, Cross-kink unpinning controls the medium-to high-temperature strength of body-centered cubic NbTiZr medium-entropy alloy. Scr. Mater. **209**, 114367 (2022)
19. O. Senkov, S. Gorsse, D.B. Miracle, High temperature strength of refractory complex concentrated alloys. Acta Mater. **175**, 394–405 (2019)
20. C. Varvenne, A. Luque, W.G. Nöhring, W.A. Curtin, Average-atom interatomic potential for random alloys. Phys. Rev. B **93**(10), 104201 (2016)
21. Y.-J. Hu, M.R. Fellinger, B.G. Butler, Y. Wang, K.A. Darling, L.J. Kecskes, D.R. Trinkle, Z.-K. Liu, Solute-induced solid-solution softening and hardening in bcc tungsten. Acta Mater. **141**, 304–316 (2017)
22. H. Li, C. Draxl, S. Wurster, R. Pippan, L. Romaner, Impact of d-band filling on the dislocation properties of BCC transition metals: The case of tantalum-tungsten alloys investigated by density-functional theory. Phys. Rev. B **95**(9), 094114 (2017)
23. X. Zhou, R. Johnson, H. Wadley, Misfit-energy-increasing dislocations in vapor-deposited CoFe/NiFe multilayers. Phys. Rev. B **69**(14), 144113 (2004)
24. A. Ghafarollahi, W.A. Curtin, unpublished work
25. S. Rao, B. Akdim, E. Antillon, C. Woodward, T. Parthasarathy, O. Senkov, Modeling solution hardening in BCC refractory complex concentrated alloys: NbTiZr, Nb1. 5TiZr0. 5 and Nb0. 5TiZr1. 5. Acta Mater. **168**, 222–236 (2019)
26. S. Rao, C. Woodward, B. Akdim, O. Senkov, D. Miracle, Theory of solid solution strengthening of BCC Chemically Complex Alloys. Acta Mater. **209**, 116758 (2021)
27. Z. Han, N. Chen, S. Zhao, L. Fan, G. Yang, Y. Shao, K. Yao, Effect of Ti additions on mechanical properties of nbmotaw and vnbmotaw refractory high entropy alloys. Intermetallics **84**, 153–157 (2017)
28. O.N. Senkov, G. Wilks, J. Scott, D.B. Miracle, Mechanical properties of nb25mo25ta25w25 and v20nb20mo20ta20w20 refractory high entropy alloys. Intermetallics **19**(5), 698–706 (2011)
29. L. Dezerald, L. Proville, L. Ventelon, F. Willaime, D. Rodney, First-principles prediction of kink-pair activation enthalpy on screw dislocations in bcc transition metals: V, Nb, Ta, Mo, W, and Fe. Phys. Rev. B **91**(9), 094105 (2015)
30. R. Kubilay, A. Ghafarollahi, F. Maresca, W. Curtin, High energy barriers for edge dislocation motion in body-centered cubic high entropy alloys. NPJ Comput. Mater. **7**(1), 1–9 (2021)
31. D. Nguyen-Manh, A. Horsfield, S. Dudarev, Self-interstitial atom defects in BCC transition metals: Group-specific trends. Phys. Rev. B **73**(2), 020101 (2006)
32. C. Lee, F. Maresca, R. Feng, Y. Chou, T. Ungar, M. Widom, K. An, J.D. Poplawsky, Y.-C. Chou, P.K. Liaw, Strength can be controlled by edge dislocations in refractory high-entropy alloys. Nat. Commun. **12**(1), 1–8 (2021)
33. R. Scattergood, D. Bacon, The Orowan mechanism in anisotropic crystals. Philos. Mag. **31**(1), 179–198 (1975)
34. L. Kubin, *Dislocations, Mesoscale Simulations and Plastic Flow*, vol. 5 (Oxford University Press, Oxford, 2013), p.240
35. F. Maresca, C. Lee, R. Feng, Y. Chou, T. Ungar, M. Widom, J. Poplawsky, Y. Chou, P. Liaw, W. Curint, Prediction of yield strength in refractory body-centered-cubic High Entropy Alloys. https://archive.materialscloud.org/record/2021.65 (2021)
36. Y.-J. Hu, Z.K. Liu, Personal Communication (2019)
37. Y. Rao, C. Baruffi, A. De Luca, C. Leinenbach, W.A. Curtin, Theory-guided design of high-strength, high-melting point, ductile, low-density, single-phase BCC high entropy alloys. Submitted to Acta Materialia
38. D. Tabor, The Hardness of Metals. Chapter 2, Clarendon. Oxford (1951)
39. E. Pavlina, C. Van Tyne, Correlation of yield strength and tensile strength with hardness for steels. J. Mater. Eng. Perform. **17**(6), 888–893 (2008)
40. Y. Tian, L. Li, J. Li, Y. Yang, S. Li, G. Qin, Correlating strength and hardness of high-entropy alloys. Adv. Eng. Mater. **23**(8), 2001514 (2021)
41. P. Zhang, S. Li, Z. Zhang, General relationship between strength and hardness. Mater. Sci. Eng.: A **529**, 62–73 (2011)
42. J.-P. Couzinié, L. Lilensten, Y. Champion, G. Dirras, L. Perrière, I. Guillot, On the room temperature deformation mechanisms of a TiZrHfNbTa refractory high-entropy alloy. Mater. Sci. Eng.: A **645**, 255–263 (2015)

Publisher's Note Springer Nature remains neutral with regard to jurisdictional claims in published maps and institutional affiliations.

Springer Nature or its licensor holds exclusive rights to this article under a publishing agreement with the author(s) or other rightsholder(s); author self-archiving of the accepted manuscript version of this article is solely governed by the terms of such publishing agreement and applicable law.